# Special Articles on 1-Gbit/s Packet Signal Transmission Experiments toward Broadband Packet Radio Access

## Experimental Equipment and Technology Overview

*Kenichi Higuchi, Noriyuki Maeda,*
*Hiroyuki Kawai and Mamoru Sawahashi*

*Experimental equipment for broadband packet radio access based on MIMO multiplexing has achieved a throughput of greater than 1 Gbit/s for a 100-MHz channel bandwidth (frequency efficiency: 10 bit/s/Hz) using up to four transmitter/receiver antenna branches. On the receiver side, this equipment has achieved high-accuracy signal detection even for low received signal power through QRM-MLD with adaptive selection of surviving symbol replica candidates based on maximum reliability .*

### 1. Introduction

For future mobile communication systems beyond the Third-Generation (3G) system, it is considered that radio access and Radio Access Networks (RANs) with a short delay (i.e., low latency) and with high affinity to Internet Protocol (IP)-based core networks are desirable. In addition, a broadband approach shows promise in providing rich high-rate services at low cost via RANs. In such a broadband channel where multipath effects are considerable, much research is focusing on radio access based on Orthogonal Frequency Division Multiplexing (OFDM) as a promising candidate [1]–[4]. In OFDM-based radio access, a broadband signal is divided into multiple subcarriers with each having a low-speed symbol rate, and multiple signals are transmitted in parallel in the frequency domain to decrease signal distortion due to frequency selective fading caused by multipaths. Members of our research group

have proposed the concept of a Variable Spreading Factor (VSF) in radio access based on Orthogonal Frequency and Code Division Multiplexing (OFCDM) and spread OFDM to achieve flexible support of various radio channel environments using the same RAN [4].

Seamless support for local areas such as very-small cells (i.e., hot-spot areas), isolated cells and indoor environments in addition to cellular cells with wide area coverage is needed for future RANs. Since the traffic density in such local areas is high in general, data rates much higher than that of cellular environments are needed. Space Division Multiplexing (SDM) that takes advantage of Multiple Input Multiple Output (MIMO) channels is very beneficial for enhancing the achievable user data rate (i.e., frequency efficiency) [5][6]. This system uses multiple transmitter and receiver antenna branches to perform spatial multiplexing of physical channels. To test this system, we have constructed experimental equipment for broadband packet radio access using MIMO multiplexing designed to achieve a maximum throughput of greater than 1 Gbit/s. This equipment applies MIMO multiplexing with four antenna branches on both the transmitter and receiver sides to achieve a throughput of greater than 1 Gbit/s for a 100-MHz channel bandwidth (frequency efficiency: 10 bit/s/Hz).

This article reports on the radio access used in our 1-Gbit/s packet transmission experiments, the technical features of the prototype experimental equipment and the signal-detection technology that plays a key role in this system.

## 2. Broadband Packet Radio Access

### 2.1 Downlink Radio Access

In framework recommendation ITU-R M.1645, the maximum data rate supported in the new mobile access scheme is defined as 100 Mbit/s and that in the new nomadic/local area radio access scheme is greater than 1 Gbit/s [7]. Based on this recommendation, we have set the maximum date rate to be greater than 100 Mbit/s for cellular environments that support wide-area coverage and high mobility and greater than 1 Gbit/s for local areas such as isolated-cell, very-small-cell (hot spots) and indoor environments. Our proposed design concept is to support both wide and local area environments using the same radio access scheme, i.e., air interference, by simply changing the radio parameters. For the downlink, we consider that the above targets are to be met for a 100-MHz channel bandwidth, which means that reducing the effects of MultiPath Interference (MPI) in such broadband transmission becomes a crucial technical issue. One effective way of reducing the effects of MPI is multi-carrier transmission, which divides a broadband signal into multiple subcarriers, each with a low-speed symbol rate and transmits these subcarrier signals in parallel. **Figure 1** shows the principle of our proposed VSF-Spread OFDM. For a cellular environment having a multi-cell configuration, one-cell frequency reuse is essential for achieving large capacity. But to achieve one-cell frequency reuse, it is necessary to suppress interference from neighboring cells so that the required Signal-to-Interference plus Noise power Ratio (SINR) can be satisfied, and for this purpose, we use spreading including channel coding. For a local area environment, on the other hand, interference from neighboring cells is relatively small, and a high data rate can be achieved by setting the spreading factor to 1 (i.e., no spreading) and making the coding rate large. Also, as signal resolution in the frequency domain is high in Orthogonal Frequency Division Multiple Access (OFDMA), frequency

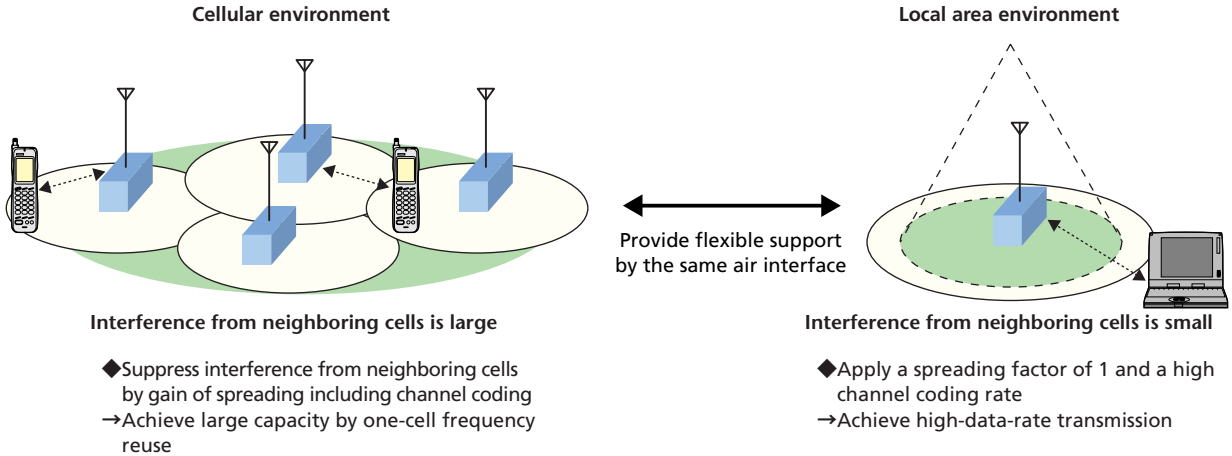


**Figure 1 Basic principle of VSF-Spread OFDM**

scheduling is performed. This process divides the entire channel bandwidth into multiple frequency blocks and allocates them to users to maximize received SINR taking the channel fluctuation of each user into account. In this way, a multi-user diversity effect can be obtained between communicating users.

### 2.2 Uplink Radio Access

In contrast to the downlink, radio access in the uplink requires that due consideration be given to limiting both transmit power and overall power consumption of the mobile terminal. The single-carrier transmission approach is advantageous for mobile terminals because its Peak-to-Average Power Ratio (PAPR) is inherently much lower compared to multi-carrier access such as OFDMA leading to lower power consumption. Consequently, under the assumption that power amplifiers have the same maximum transmit power, transmit back-off can be lowered and a wide coverage area can be achieved. For the above reasons, the radio access used for the uplink is a single-carrier type using spreading with channel coding. Here, to achieve one-cell frequency reuse, we apply Turbo coding to part of the spreading. While single-carrier-based radio access is advantageous over multi-carrier access from the viewpoint of lowering PAPR, the effective spreading factor is 1 in packet transmission, and as a result, SINR is very low due to MPI effects. As a consequence, high-accuracy signal detection cannot be achieved in MIMO multiplexing because of large interference power, making it necessary here to apply a MultiPath Interference Canceller (MPIC) before signal detection to reduce MPI.

## 3. Overview of Experimental Equipment

### 3.1 Radio Frame Configuration

The MIMO experimental equipment that we constructed targets packet access. It adopts Adaptive Modulation and channel Coding (AMC) and hybrid Automatic Repeat reQuest (ARQ) suitable for packet signal transmission. To achieve a short control delay for these key technologies, Round Trip Time (RTT) is set to 0.5 ms, the same as the Transmission Time Interval (TTI), the unit of packet transmission.

In MIMO multiplexing, each of the transmitter antenna branches transmits a different data stream using the same radio resources. These data streams must be detected in the received signal at the receiver, and this is accomplished by using the differences in channel fluctuation between each of the transmitter antenna branches and each of the receiver antenna branches. High-accuracy signal detection therefore requires high-accuracy estimation of this channel fluctuation between the transmitter and receiver antenna branches. For this purpose, pilot symbols of the Time Division Multiplexing (TDM) type are arranged consecutively as shown in **Figure 2**. But within the short 0.5-ms TTI used here, channel fluctuation is small except times of high mobility, while for frequency-selective-fading channels, channel fluctuation in the frequency direction is large. Accordingly, the more appropriate scheme for high-accuracy channel estimation is TDM and Code Division Multiplexing (CDM) that arranges many pilot symbols in the frequency direction as opposed to Frequency Division Multiplexing (FDM) that arranges many pilot symbols in the time direction. In a CDM-type configuration, inter-code interference occurs from code-multiplexed data symbols, and in MIMO multiplexing, in particular, the accuracy of channel estimation deteriorates slightly compared to a TDM configuration. In these experiments, we used a TDM-type of pilot channel configuration.

For the uplink, in contrast, we used a code-multiplexed CDM-type pilot-channel configuration for the data channel. In comparison to the TDM type, the CDM type, while exhibiting large MPI from the data channels, allows for accumulation of pilot symbols across one TTI interval enabling received SINR to be improved through processing gain (in the TDM configuration, the pilot interval is short and an averaged interval cannot usually be obtained). The CDM type, moreover, allows pilot power to be changed flexibly in accordance with the data rate of

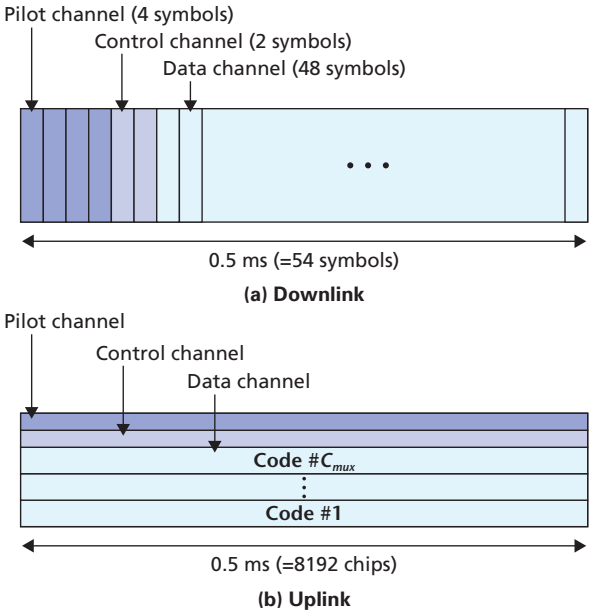


**Figure 2 Frame configuration**

the data channel and enables efficient allocation of pilot power according to the data rate. In a TDM configuration, the pilot-symbol interval is fixed and peak power increases when changing pilot-symbol power according to data rate. A CDM configuration, however, adopts an MPIC before signal detection in MIMO multiplexing as described later. This can produce undesirable effects from erroneous decoding of data symbols unlike a TDM-type configuration.

### 3.2 Technical Features of Experimental Equipment for Broadband Packet Radio Access

The following describes the technical features of equipment constructed for experiments in broadband packet radio access using MIMO multiplexing.

1) Application of a Maximum Likelihood Detection (MLD)-Based Signal Detection Method

As shown in **Table 1**, there are three main methods for performing signal detection in MIMO multiplexing. These are the linear filter method based on a two-dimensional Minimum Mean Squared Error (MMSE) method in the space and time domains, the Vertical Bell laboratories LAyered Space-Time (V-BLAST) method that performs successive decoding starting with the transmit signal with the largest received SINR by generating a transmit-signal replica and applying a serial interference canceller [8] and the MLD method [9]. Though the MMSE and V-BLAST methods can reduce computational complexity, required SINR is much larger than that of MLD for the same received quality as explained in this special article in "Configuration and Performances of Implemented Experimental Equipment." In particular, the area in which multi-value modulation like 16 Quadrature Amplitude Modulation (16QAM) can be used in conjunction with MMSE and V-BLAST is extremely limited. For this reason, we decided to use an MLD-based signal detection method. **Figure 3** shows the operating principle of the MLD method. Here, to simplify the following discussion, we assume the use of Quadrature Phase Shift Keying (QPSK) with two antenna branches on both the transmitter and receiver sides. The MLD method estimates channel fluctuation on the pilot channel between the transmitter and receiver antenna branches, and by using the value of channel fluctuation so estimated (channel estimation value), it creates a data-modulation constellation for each transmit signal and prepares symbol replica candidates that combine all of the transmit signals. As shown in Fig. 3, four signal points are possible for each transmit signal in QPSK modulation, and because two transmit signals are combined here, a total of $4^2$=16 signal points can be considered. The distances (squared Euclidian distances) between these 16 received symbol replica candidates and actually received signal points are compared, and the combination of transmitted symbol combination having the smallest squared Euclidian distance is used to determine data modulation for each transmit signal. This process implies that the number of symbol replica candidates for which squared Euclidian distances must be computed will increase dramatically with increase in data modulation points and number of transmitter antenna branches. Such a large degree of computational complexity creates a processing bottleneck in practice. (To give an example, 16QAM data modulation with four transmitter antenna branches results in the creation of $16^4$=65,536 transmit symbol replica candidates at the receiver. The squared Euclidian distance between each symbol replica and the received signal must be calculated.) In response to this problem, complexity-reduced Maximum Likelihood Detection with QR decomposition and M-algorithm (QRM-MLD) [10] has been proposed as a method for reducing the huge volume of computational complexity in conventional MLD. And based on this QRM-MLD method, the Adaptive SElection of Surviving Symbol replica candidates based on maximum reliability (ASESS) method [11] has also been proposed. This method, while achieving nearly the same packet error rate and throughput characteristics as conventional MLD having no reduction in

**Table 1 Comparison of signal detection methods**

| | Features | Computational complexity |
|---|---|---|
| MLD | • Good signal detection characteristics (for channel detection of the same frequency, slot and code)<br>→ Reduces required average received $E_b/N_0$ (signal energy per bit-to-noise power spectrum density ratio)<br>→ Achieves high throughput | Very large |
| V-BLAST | • Performs successive decoding by creating transmit signal replicas and applying serial interference cancellers<br>• Signal-detection characteristics are inferior to those of MLD | Medium |
| MMSE | • A linear-filter method based on the MMSE<br>• Signal-detection characteristics are inferior to those of MLD and V-BLAST | Small |

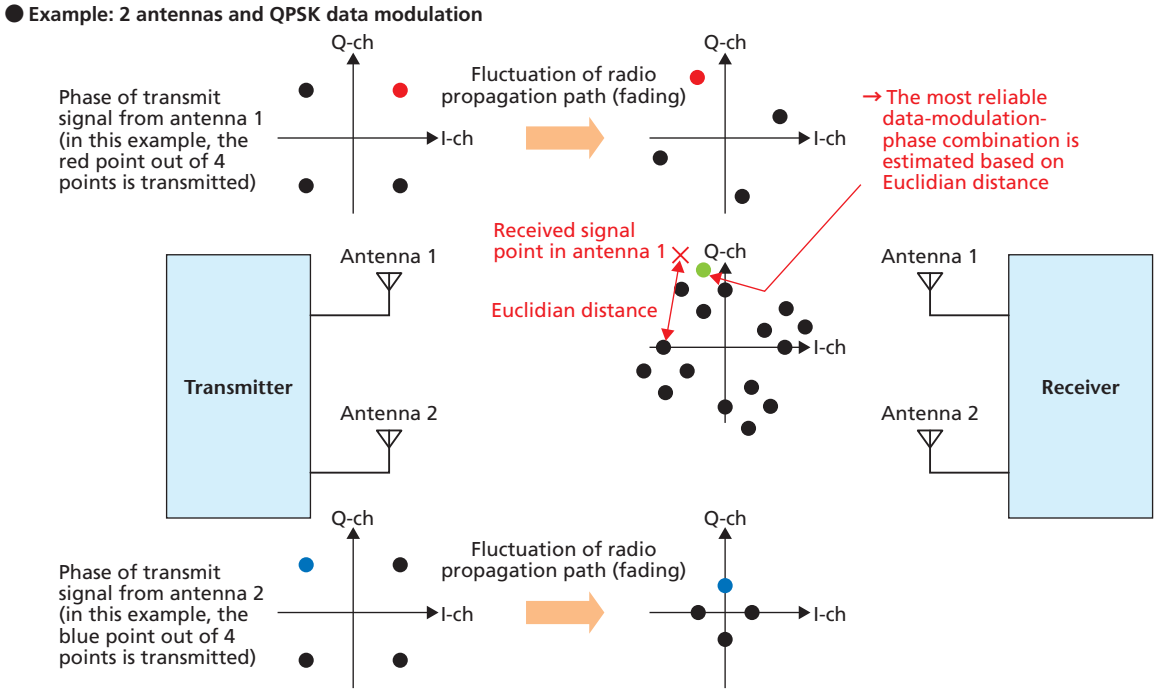


**Figure 3 Principle of the MLD method**

computational complexity (hereinafter referred to as Full MLD), has been shown to reduce computational complexity (considering all multiplication, addition and comparison operations required for signal detection) to about 1/1200 that of Full MLD and about 1/4 that of the original QRM-MLD method. By using this QRM-MLD signal-detection method with ASESS, our experimental equipment has demonstrated real-time transmission at a data rate of 1 Gbit/s (frequency efficiency: 10 bit/s/Hz).

2) Application of a Multi-Slot and sub-Carrier Averaging (MSCA) Channel Estimation Filter

The accuracy of signal detection in MIMO multiplexing/diversity strongly depends on the accuracy of channel estimation between the transmitter and receiver antenna branches. Taking this into account, the experimental equipment applies a channel estimation filter based on MSCA [12]. This filter performs multi-slot and subcarrier two-dimensional-weighted averaging using a time-multiplexed-orthogonal pilot channel. It carries out channel estimation using many pilot symbols from multiple TTIs in the time domain and from multiple adjacent subcarriers in the frequency domain. This makes for high-accuracy channel estimation in which the effects of noise are small. However, as the use of pilot symbols from TTIs and subcarriers for which channel fluctuation is large and fading correlation is small will only degrade the accuracy of channel estimation, the approach taken here is to perform weighted averaging using weighted coefficients taking fading correlation into account.

3) Generation of Likelihood Function for Soft-Decision Turbo Decoding

In Wideband Code Division Multiple Access (W-CDMA) in which Turbo coding is applied, soft-decision decoding is essential for obtaining large coding gain. Here, soft-decision decoding requires a Log Likelihood Ratio (LLR) of *A Posteriori* Probability (APP) for each bit "1" and "–1." The QRM-MLD method, however, successively reduces the number of surviving symbol replica candidates for which squared Euclidian distance must be calculated. Thus, as shown in **Figure 4**, the case may arise that either a "1" or "–1" information bit may not exist in a certain bit position in the symbol replica candidates that have survived up to the final stage of this process. This experimental equipment therefore incorporates the method proposed in Ref. [13] for estimating LLR required for soft-decision decoding in such a situation.

4) AMC Applied to MIMO Multiplexing

As shown in **Figure 5**, this experimental equipment applies a method that independently controls a Modulation and channel Coding Scheme (MCS) for each transmitter antenna branch based on the measurement of instantaneous received SINR for that branch. The equipment can perform high-speed, optimal MCS selection at every 0.5-ms TTI.

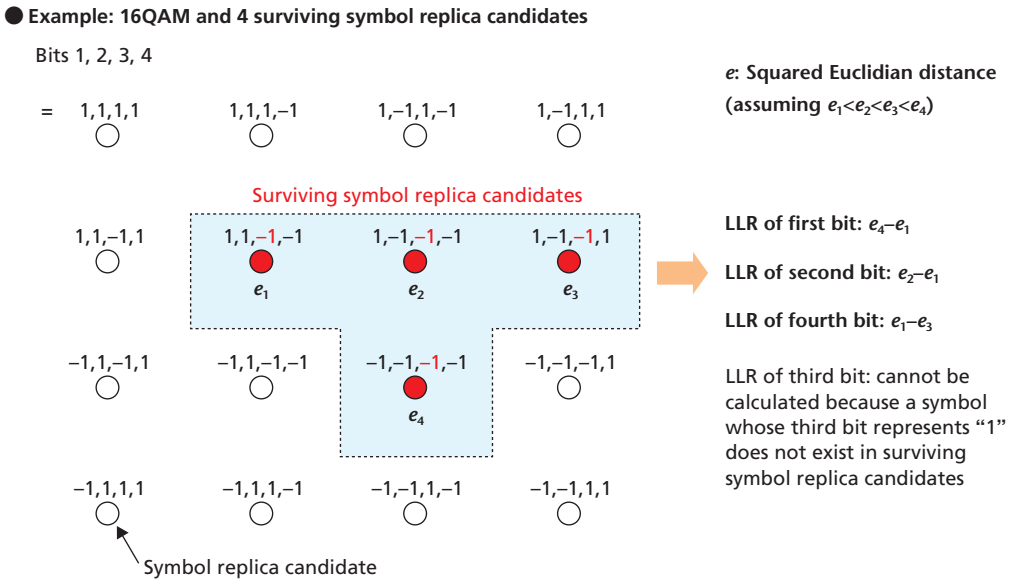


**Figure 4 Necessity of likelihood calculation for a non-existing bit**

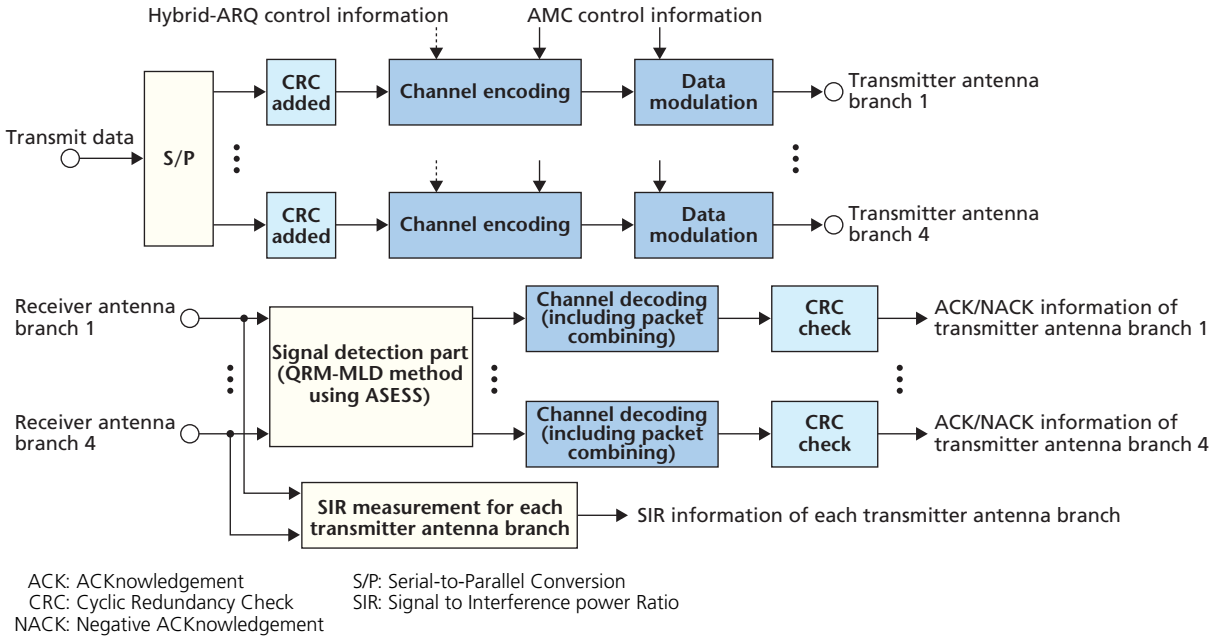


**Figure 5 Control of AMC and hybrid ARQ in MIMO multiplexing**

5) Hybrid ARQ Applied to MIMO Multiplexing

A repeat-request scheme is essential for achieving high-quality packet access. This experimental equipment achieves independent repeat-request control for each transmitter antenna branch by checking for packet errors every TTI of each transmit signal (Fig. 5). A packet-combining type of hybrid ARQ is used here for repeat-request control.

6) Transmission Control Protocol/Internet Protocol (TCP/IP) Interface

A TCP/IP interface is used between external applications terminals and our experimental equipment using MIMO multiplexing. By using MIMO multiplexing with up to four transmitter/receiver antenna branches having the technical features described above and applying 16QAM modulation and Turbo coding with a channel coding rate of 8/9, a maximum throughput of 1 Gbit/s is achieved for a 100-MHz channel bandwidth.

## 4. Signal Detection Methods

### 4.1 Signal Detection Method in Downlink OFDM Access

1) QRM-MLD Signal Detection Method

We consider MIMO multiplexing with four transmitter/receiver antenna branches. Let $\mathbf{X}_k=[x_{1,k}, x_{2,k}, x_{3,k}, x_{4,k}]^T$ denote the trans-

mit signals from the four transmitter antenna branches for $k$th subcarrier and $\mathbf{Y}_k=[y_{1,k}, y_{2,k}, y_{3,k}, y_{4,k}]^T$ the received signals at the four receiver antenna branches for $k$th subcarrier (here, the notation for the temporal waveform is omitted). Now, letting $h_{m,n,k}$ denote the channel fluctuations between transmitter antenna branches $m$ ($1\leq m\leq 4$) and receiver antenna branches $n$ ($1\leq n\leq 4$) for $k$th subcarrier, we get the following equation for the received signals.

$$\mathbf{Y}_k=\mathbf{H}_k\mathbf{X}_k+\mathbf{N}_k$$

$$\begin{bmatrix} y_{1,k} \\ y_{2,k} \\ y_{3,k} \\ y_{4,k} \end{bmatrix} = \begin{bmatrix} h_{1,1,k} & h_{2,1,k} & h_{3,1,k} & h_{4,1,k} \\ h_{1,2,k} & h_{2,2,k} & h_{3,2,k} & h_{4,2,k} \\ h_{1,3,k} & h_{2,3,k} & h_{3,3,k} & h_{4,3,k} \\ h_{1,4,k} & h_{2,4,k} & h_{3,4,k} & h_{4,4,k} \end{bmatrix} \begin{bmatrix} x_{1,k} \\ x_{2,k} \\ x_{3,k} \\ x_{4,k} \end{bmatrix} + \begin{bmatrix} n_{1,k} \\ n_{2,k} \\ n_{3,k} \\ n_{4,k} \end{bmatrix} \quad (1)$$

In equation (1), $\mathbf{H}_k$ is a $4\times 4$ matrix having as elements the channel-fluctuation values between the transmitter and receiver antenna branches for $k$th subcarrier (referred to below as the "channel matrix"). $\mathbf{N}_k=[n_{1,k}, n_{2,k}, n_{3,k}, n_{4,k}]^T$ denotes the noise component of each receiver branch for $k$th subcarrier. As indicated by equation (1), each received signal at each antenna branch combines the transmit signals emitted from multiple transmitter antenna branches (corresponding to a state of same-channel interference). Detecting these signals by MLD would require the generation of a huge number of transmit symbol replica candidates.

In the QRM-MLD method, $\mathbf{Q}_k$ denotes an $N_r\times N_t$ unitary matrix (where $N_r$ and $N_t$ denote the numbers of receiver and transmitter antenna branches, respectively, with the maximum value of each being 4 in this experimental equipment). Using $\mathbf{Q}_k$, the estimation values of the channel matrix of equation (1) can be subjected to QR decomposition as in $\hat{\mathbf{H}}_k=\mathbf{Q}_k\bullet\mathbf{R}_k$ to obtain an $N_t\times N_t$ upper triangular matrix as shown by the following equation for $\mathbf{R}_k$.

$$\mathbf{R}_k=\mathbf{Q}_k^H\hat{\mathbf{H}}_k = \begin{bmatrix} r_{1,1,k} & r_{1,2,k} & r_{1,3,k} & r_{1,4,k} \\ 0 & r_{2,2,k} & r_{2,3,k} & r_{2,4,k} \\ 0 & 0 & r_{3,3,k} & r_{3,4,k} \\ 0 & 0 & 0 & r_{4,4,k} \end{bmatrix} \quad (2)$$

Here, by multiplying $\mathbf{Q}_k^H$ (where $H$ denotes a Hermitian transpose) by received signal $\mathbf{Y}_k$ of each OFDM subcarrier, the signal at each receiver antenna branch can be expressed by the product of upper triangular matrix $\mathbf{R}_k$ and transmit-signal vector $\mathbf{X}_k$ as shown by equation (3).

$$\mathbf{Z}_k=\begin{bmatrix} z_{4,k} \\ z_{3,k} \\ z_{2,k} \\ z_{1,k} \end{bmatrix}=\mathbf{Q}_k^H\mathbf{Y}_k=\mathbf{Q}_k^H\begin{bmatrix} y_{1,k} \\ y_{2,k} \\ y_{3,k} \\ y_{4,k} \end{bmatrix}=\mathbf{R}_k\mathbf{X}_k+\mathbf{W}_k$$

$$=\begin{bmatrix} r_{1,1,k} & r_{1,2,k} & r_{1,3,k} & r_{1,4,k} \\ 0 & r_{2,2,k} & r_{2,3,k} & r_{2,4,k} \\ 0 & 0 & r_{3,3,k} & r_{3,4,k} \\ 0 & 0 & 0 & r_{4,4,k} \end{bmatrix}\begin{bmatrix} x_{1,k} \\ x_{2,k} \\ x_{3,k} \\ x_{4,k} \end{bmatrix}+\begin{bmatrix} w_{1,k} \\ w_{2,k} \\ w_{3,k} \\ w_{4,k} \end{bmatrix} \quad (3)$$

Here, $\mathbf{W}_k=\mathbf{Q}_k^H\mathbf{N}_k$. In this equation, since $\mathbf{R}_k$ is an upper triangular matrix as described above, $z_{1,k}$ is expressed by only transmit signal $x_{4,k}$ indicating that nulling (orthogonalization) can be achieved. Similarly, $z_{2,k}$ is expressed by only $x_{3,k}$ and $x_{4,k}$, and $z_{3,k}$ by $x_{2,k}$, $x_{3,k}$ and $x_{4,k}$. This is a feature resulting from the QR decomposition of the channel matrix into unitary matrix $\mathbf{Q}_k$ and upper triangular matrix $\mathbf{R}_k$.

Next, we describe a method for selecting surviving symbol replica candidates using the M-algorithm. In the following, we omit subcarrier number $k$.

In the first stage ($m$=1), the process begins by generating all symbol replica candidates $c_x$ of transmit signal 1 (where $1\leq x\leq C$ and $C$ is the number of symbol constellations, which is 4 for QPSK modulation and 16 for 16QAM modulation) and calculating the squared Euclidian distance between $z_1$ and $c_x$ (called a branch metric in the sense that it represents reliability). The branch metrics so obtained are now compared for all symbol replica candidates and $S_1$ ($S_1\leq C$) surviving symbol replica candidates $c_{m=1,1},\ldots, c_{1,S_1}$ are selected in order of smallest to larger branch-metric values. The branch metrics $E_{m=1,1},\ldots, E_{1,S_1}$ corresponding to these surviving symbol replica candidates are saved at this time. Here, since no interference signal components of transmit signals 2,..., $N_t$ are included in $z_1$, symbol replica candidates for transmit signal 1 can be selected with high accuracy.

In the second stage, with respect to all ($S_1C$) combinations of $S_1$ surviving symbol replica candidates $c_{1,1},\ldots, c_{1,S_1}$ for transmit signal 1 and all symbol replica candidates $c_x$ for transmit signal 2, the process updates accumulated branch metrics based on the squared Euclidian distances for the $c_x$ combinations between $z_2$ and symbol replica candidates $c_{1,y}$ ($1\leq y\leq S_1$) and on the branch metrics of surviving symbol replica candidates from the first stage. Similar to the first stage, the surviving symbol replica candidates selected in this stage are taken to be the $S_2$ ($S_2\leq S_1C$) transmit-signal-1 and transmit-signal-2 symbol-replica-candidate combinations $\mathbf{c}_{m=2,1}=[c_{m=2,1,2}, c_{2,1,1}]^T,\ldots, \mathbf{c}_{2,S_2}=[c_{2,S_2,2}, c_{2,S_2,1}]^T$ in order

of smallest to larger accumulated-branch-metric values. Here as well, the process saves the corresponding accumulated branch metrics $E_{2,1}$,..., $E_{2,S_2}$. This process is repeated so that the system eventually outputs, at the $N_t$ stage, $S_{N_t-1}C$ combinations of surviving symbol replica candidates for all transmit signals plus the corresponding accumulated branch metrics. If using the original QRM-MLD method given in Ref. [10], the number of times that squared Euclidian distance would have to be calculated would be $C$ times in stage 1 and $S_{m-1}C$ times in stage $m$ ($m$>1) for a total of $(1+\sum_{m=1}^{N_t-1}S_m)C$ calculations, which represents a reduction in computational complexity.

2) ASESS

Although the QRM-MLD method can significantly reduce computational complexity compared to the MLD method, it must calculate the squared Euclidian distance for all surviving symbol replica candidates in each stage making for high computational complexity compared, for example, to the MMSE method. We therefore proposed a method for ASESS to reduce computational complexity even further. **Figure 6** shows the basic principle of ASESS, which consists of the following two steps.

- Step 1

  At stage $m$, rank the reliability of $C$ symbol replica candidates of the newly added transmit signal by quadrant detection for each surviving symbol replica candidate of the previous stage ($m$–1).

- Step 2

  Apply repeat control to adaptively select the $S_m$ surviving symbol replica candidates to be passed on to the next stage (after stage $m$). "Repeat control" makes use of reliability information consisting of accumulated branch metrics of the $S_{m-1}$ surviving symbol replica candidates from the previous stage, and the ranking results of the $C$ surviving symbol replica candidates added in the present stage. By repeat processing, the surviving symbol replica candidate with the highest reliability can be selected each time. Note here that a branch metric is calculated for a selected symbol replica candidate based on the squared Euclidian distance between it and the received signal point, and that this branch metric is added to the accumulated branch metric every stage up to stage $m$ to update that accumulated value.

In short, as the squared Euclidian distance needs to be calculated for only the $S_m$ symbol replicas with highest reliability out of a total of $S_{m-1}C$ symbol replicas, ASESS achieves nearly the same throughput as the Full MLD method while reducing computational complexity (considering all multiplication, addition and comparison operations required for signal detection) to about 1/1200 that of Full MLD and about 1/4 that of the original QRM-MLD method.

### 4.2 Signal Detection Method in Uplink DS-CDMA Access

The uplink adopts Direct Sequence-Code Division Multiple Access (DS-CDMA) for radio access. The data channel features a spreading factor of 16 and 15-codes multiplexing to achieve a high data rate. But the effective spreading factor, as a consequence, is 15/16≈1, which means that there is no spreading gain and MPI cannot be suppressed. Received SINR is therefore very small due to MPI from both a single transmitter antenna branch and different transmitter antenna branches as shown in **Figure 7**. This MPI prevents sufficient direct signal detection of the received signal even if the QRM-MLD method used in the downlink were to be applied.

This is addressed by applying QRM-MLD using a three-stage MPIC in the experimental equipment [14]. **Figure 8** shows the configuration of the signal detection part in a base station receiver. It consists of an MPIC block that makes use of

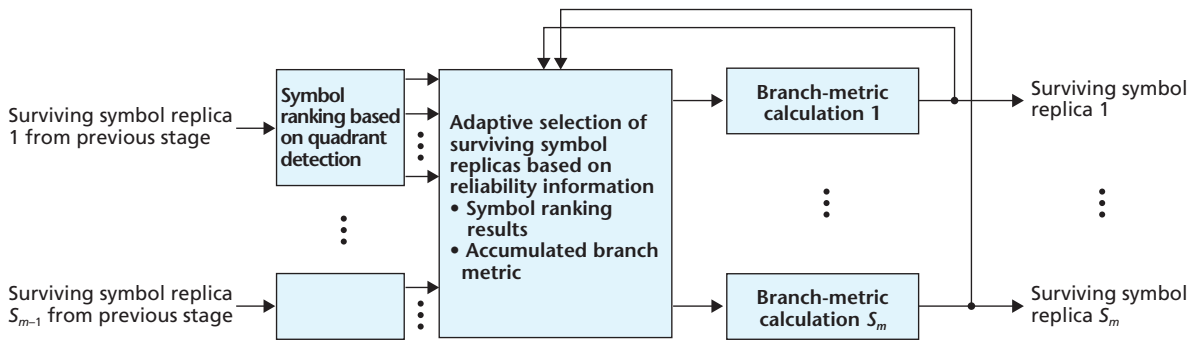


**Figure 6 Principle of ASESS**

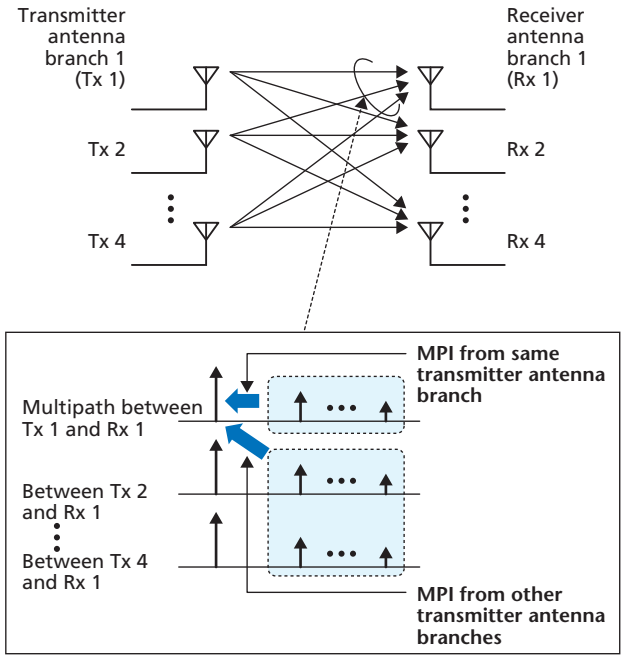


**Figure 7 Effects of MPI in broadband DS-CDMA MIMO multiplexing**

temporary signal detection results based on two-dimensional MMSE filters, and a signal detection block based on the QRM-MLD method. First, using the received timing of each path estimated by pilot symbols, the first stage MPI-replica generator performs accumulation of the pilot symbols after despreading in one frame to determine channel estimation value $\hat{\xi}_{p,q,l}^{(1)}$ in path $l$ between transmitter antenna branch $p$ and receiver antenna branch $q$ (the superscript (1) here indicates a first stage value). The two-dimensional-MMSE equalizer here applies a Fast Fourier Transform (FFT) at $N_{\mathrm{FFT}}$ points with respect to the channel estimation value $\hat{\xi}_{p,q,l}^{(1)}$ obtained above and calculates $N_r \times N_t$ frequency-domain channel matrix $\hat{\mathbf{H}}_f^{(1)}=[\hat{h}_{p,q,f}^{(1)}]$ for $f$th subcarrier ($0 \le f \le N_{\mathrm{FFT}}$). A weighted matrix consisting of two-dimensional MMSE weights from this channel matrix can be expressed by the following equation:

$$\mathbf{W}_f^{(1)}=(\hat{\mathbf{H}}_f^{(1)})\{\hat{\mathbf{H}}_f^{(1)}(\hat{\mathbf{H}}_f^{(1)})^H+\mathbf{N}_f\mathbf{I}\}^{-1} \quad (4)$$

In equation (4), $\mathbf{N}_f$ represents residual interference and noise components. Next, denoting the received signal after conversion by FFT at $N_{\mathrm{FFT}}$ points as $\hat{\mathbf{Y}}_f=[y_{q,f}]^T$, the signal is equalized by two-dimensional MMSE expressed as $\hat{\mathbf{X}}_f^{(1)}=(\mathbf{W}_f^{(1)})^H\mathbf{Y}_f^{(1)}$ using $\mathbf{W}_f^{(1)}$ of equation (4) obtaining post-equalization signal $\hat{\mathbf{X}}_f^{(1)}=[\hat{x}_{p,f}^{(1)}]^T$. Signal $\hat{\mathbf{X}}_f^{(1)}$ is then transformed to the time domain by an Inverse Fast Fourier Transform (IFFT) at $N_{\mathrm{FFT}}$ points and each soft-decision data symbol series for each code channel is generated using the despread signal [15]. A received signal replica is now generated from the soft-decision data symbols of each code channel and subtracted from the received signal. Here, when the received signal replica can be ideally estimated from the data channel, the signal remaining after subtraction is simply the pilot channel. Thus, as MPI from all transmitter antenna branches is eliminated, the accuracy of channel estimation using the pilot channel is greatly improved. Next, from the second stage MPI replica generator on, an updated channel estimation value can be used to again calculate two-dimensional MMSE weights from equation (4). Accordingly, a channel-estimation update process, which consists of two-dimensional MMSE equalization in the frequency domain followed by the generation of received signal replica for each transmitter antenna branch and each code channel using temporary post-equalization data symbols and the subtraction of that replica from the received signal, can be repeated over several stages to generate high-accuracy MPI replica.

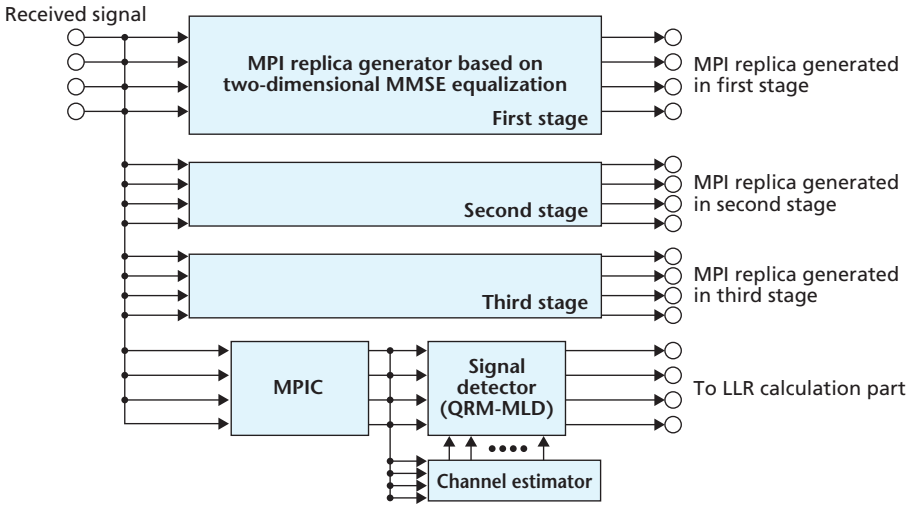


**Figure 8 Configuration of QRM-MLD signal detection using a three-stage MPIC**

The output from the three-stage MPI replica generator consists of high-accuracy channel-estimation values for each path between the transmitter and receiver antennas as well as MPI-eliminated received signals of a number equal to the number of receiver antenna branches times number of paths. In other words, while the dimension of the received spectrum of OFDM shown in equation (1) is equal to the number of receiver antenna branches, that for DS-CDMA access is equal to the number of receiver

antenna branches times number of paths. Likewise, in contrast to the channel matrix for OFDM access shown by equation (1), the row dimension of the channel matrix for DS-CDMA access is equal to the number of receiver antenna branches times number of paths with the channel matrix itself consisting of channel estimation values for each path between the transmitter and receiver antenna branches. Also, as in the case of OFDM access, the channel matrix for DS-CDMA can be decomposed into unitary matrix **Q** and upper triangular matrix **R**, and the Hermitian transpose of the **Q** matrix can be multiplied by the received signal vector to achieve orthogonalization between the transmitter antenna branches. In addition, the process of multiplying the Hermitian transpose of the **Q** matrix by the received signal vector obtains a path diversity effect equivalent to subjecting the path signals to Rake combining. The rest of QRM-MLD processing is the same as that of OFDM access in the downlink.

## 5. Conclusion

This article described the radio access used in 1-Gbit/s packet transmission experiments, the technical features of the prototype experimental equipment constructed for these experiments and the signal-detection technology that plays a key role in this system. Main features are as follows.

- MIMO multiplexing with up to four transmitter/receiver antenna branches achieving a maximum throughput of 1-Gbit/s for a 100-MHz channel bandwidth (assuming 16QAM modulation and Turbo coding with a channel coding rate of 8/9)
- QRM-MLD signal detection using adaptive selection of surviving symbol replica candidates based on maximum reliability
- Independent adaptive modulation/demodulation, channel coding and hybrid ARQ for each transmitter antenna branch
- Total packet access for highly efficient TPC/IP transmission

For the future, we plan to perform both laboratory and field experiments to continue evaluating the characteristics of 1-Gbit/s packet transmission using MIMO multiplexing in broadband packet radio access.

### References


[1] T. A. Thomas, K. L. Baum and F. W. Vook: "Modulation and coding rate selection to improve successive cancellation reception in OFDM and spread OFDM MIMO systems," Proc. IEEE ICC 2003, pp. 2842–2846, May 2003.

[2] N. Yee, J.-P. Linnartz and G. Fettweis: "Multi-Carrier CDMA in indoor wireless radio networks," Proc. PIMRC '93, pp. 109–113, Sep. 1993.

[3] K. Fazel and L. Papke: "On the performance of convolutional-coded CDMA/OFDM for mobile communication systems," Proc. PIMRC '93, pp. 468–472, Sep. 1993.

[4] H. Atarashi, S. Abeta and M. Sawahashi: "Variable spreading factor orthogonal frequency and code division multiplexing (VSF-OFCDM) for broadband packet wireless access," IEICE Trans. Commun., Vol. E86-B, No. 1, pp. 291–299, Jan. 2003.

[5] G. J. Foschini, Jr.: "Layered space-time architecture for wireless communication in a fading environment when using multi-element antennas," Bell Labs Tech. J., pp. 41–59, Autumn 1996.

[6] R. D. Murch and K. B. Letaief: "Antenna Systems for Broadband Wireless Access," IEEE Commun. Mag., Vol. 40, No. 4, pp. 76–83, Apr. 2002.

[7] Recommendation ITU-R M. 1645: "Framework and overall objectives of the future development of IMT-2000 and systems beyond IMT-2000."

[8] P. W. Wolniansky, G. J. Foschini, G. D. Golden and R. A. Valenzuela: "V-BLAST: an architecture for realizing very high data rates over the rich-scattering wireless channel," Proc. 1998 URSI International Symposium on Signals, Systems, and Electronics, pp. 295–300, Sep. 1998.

[9] A. van Zelst, R. van Nee and G. A. Awater: "Space division multiplexing (SDM) for OFDM systems," Proc. IEEE VTC2000-Spring, pp. 1070–1074, May 2000.

[10] K. J. Kim, J. Yue, R. A. Iltis and J. D. Gibson: "A QRD-M/Kalman filter-based detection and channel estimation algorithm for MIMO-OFDM systems," IEEE Trans. Wireless Commun., Vol. 4, No. 2, pp. 710–721, Mar. 2005.

[11] K. Higuchi, H. Kawai, N. Maeda and M. Sawahashi: "Adaptive Selection of Surviving Symbol Replica Candidates Based on Maximum Reliability in QRM-MLD for OFCDM MIMO Multiplexing," Proc. IEEE Globecom 2004, pp. 2480–2486, Nov. 2004.

[12] H. Kawai, K. Higuchi, N. Maeda and M. Sawahashi: "Performance of QRM-MLD employing two-dimensional multi-slot and carrier-averaging channel estimation using orthogonal pilot channel for OFCDM MIMO multiplexing in multipath fading channel," Proc. Wireless2004, pp. 208–214, Jul. 2004.

[13] K. Higuchi, H. Kawai, N. Maeda, M. Sawahashi, T. Itoh, Y. Kakura, A. Ushirokawa and H. Seki: "Likelihood function for QRM-MLD suitable for soft-decision turbo decoding and its performance for OFCDM MIMO multiplexing in multipath fading channel," Proc. IEEE PIMRC2004, pp. 1142–1148, Sep. 2004.

[14] N. Maeda, K. Higuchi, J. Kawamoto, M. Sawahashi, M. Kimata and S. Yoshida: "QRM-MLD combined with MMSE-based multipath interference canceller for MIMO multiplexing in broadband DS-CDMA," Proc. IEEE PIMRC2004, pp. 1741–1746, Sep. 2004.

[15] J. Kawamoto, H. Kawai, N. Maeda, K. Higuchi and M. Sawahashi: "Investigation on likelihood function for QRM-MLD combined with MMSE-based multipath interference canceller suitable for soft-decision turbo decoding in broadband CDMA MIMO multiplexing," Proc. IEEE ISSSTA 2004, pp. 628–633, Sep. 2004.

## ABBREVIATIONS

ACK: ACKnowledgement
AMC: Adaptive Modulation and channel Coding
ARQ: Automatic Repeat reQuest
CDM: Code Division Multiplexing
CRC: Cyclic Redundancy Check
DS-CDMA: Direct Sequence-Code Division Multiple Access
FDM: Frequency Division Multiplexing
FFT: Fast Fourier Transform
IFFT: Inverse Fast Fourier Transform
IP: Internet Protocol
LLR: Log Likelihood Ratio
MCS: Modulation and channel Coding Scheme
MIMO: Multiple Input Multiple Output
MLD: Maximum Likelihood Detection
MMSE: Minimum Mean Squared Error
MPI: MultiPath Interference
MPIC: MultiPath Interference Canceller
MSCA: Multi-Slot and sub-Carrier Averaging
NACK: Negative ACKnowledgement
OFCDM: Orthogonal Frequency and Code Division Multiplexing
OFDM: Orthogonal Frequency Division Multiplexing
OFDMA: Orthogonal Frequency Division Multiple Access
PAPR: Peak-to-Average Power Ratio
QAM: Quadrature Amplitude Modulation
QPSK: Quadrature Phase Shift Keying
QRM-MLD: complexity-reduced Maximum Likelihood Detection with QR decomposition and M-algorithm
RAN: Radio Access Network
RTT: Round Trip Time
S/P: Serial-to-Parallel Conversion
SDM: Space Division Multiplexing
SINR: Signal-to-Interference plus Noise power Ratio
SIR: Signal to Interference power Ratio
TCP/IP: Transmission Control Protocol/Internet Protocol
TDM: Time Division Multiplexing
TTI: Transmission Time Interval
V-BLAST: Vertical Bell laboratories LAyered Space-Time
VSF: Variable Spreading Factor
W-CDMA: Wideband Code Division Multiple Access